Carbazole derivatized n-alkyl methacrylate polymeric memristors as flexible synaptic substitutes

Carbazole Derivatized n-Alkyl Methacrylate Polymeric Memristors as Flexible Synaptic Substitutes

Tucker McFarlane, Yuriy Bandera, Benjamin Grant, Bogdan Zdyrko, Stephen H. Foulger,* Jarmila Vilčáková, Petr Sáha, and Jiří Pfleger

Dr. T. McFarlane, Dr. Y. Bandera, B. Grant, Dr. B. Zdyrko, Prof. S. H. Foulger Center for Optical Materials Science and Engineering Technologies Department of Materials Science and Engineering Clemson University Clemson, SC 29634-0971, USA

E-mail: foulger@clemson.edu

Dr. T. McFarlane Center for Optical Materials Science and Engineering Technologies Sonoco Institute of Packaging Design and Graphics Clemson University Clemson, SC 29634-0971, USA

Prof. S. H. Foulger Center for Optical Materials Science and Engineering Technologies Department of Bioengineering Clemson University Clemson, SC 29634-0971, USA

Prof. J. Vilčáková, Prof. P. Sáha Centre of Polymer Systems Tomas Bata University Zlin 760 01, Czech Republic

Dr. J. Pfleger Department of Polymers for Electronics and Photonics Institute of Macromolecular Chemistry of the Czech Academy of Sciences Prague 6 162 06, Czech Republic

ABSTRACT

A memristor is a two-terminal electronic device whose observed conductance is dependent on the history of the voltage that has been applied across the device. In this effort, poly(11-(9H-carbazol-9-yl)undecyl methacrylate) (PUMA) is fabricated into a two-terminal device with Al and ITO electrodes and exhibits a number of signature memristor characteristics such as an irreversible transition from an insulator to a conductor at a specific DC voltage and hysteresis in the AC response. A PUMA-based device could transition through a multitude of conductance states with varying voltage, allowing the device to exhibit spike-timing-dependent-plasticity, an essential feature in replicating the behavior of biological synapses.

Keywords: carbazole, memristors, n-alkyl methacrylate, spike-timing dependent plasticity

1. Introduction

A fourth passive two-terminal circuit element that could alter its conductivity based on previously applied electrical fields was proposed back in the early 1970's and was referred to as a memory resistor or "memristor"[1] and a recent theoretical review[2] has attempted to establish the unifying characteristics of these systems. Not until 2008 was a memristive device realized by Hewlett Packard which employed TiO2.[3] Nonetheless, on closer inspection of the literature, there were numerous earlier published reports with similar behaving devices but they were not recognized as memristors.[4-6] The device presented by Hewlett Packard exhibited only two conductivity states and was termed a bistable device. While this device is categorized as a mem-ristor, for a memristor to achieve relevance in synaptic memory emulation, a device would need to be created that can reversibly alter its

conductivity through a multitude of states.[7] Currently, chalcogenide glass based devices that alter the conductivity of the device through the reversible crystallization of the chalcogenide glass layer dominate the field with high switching speeds and consistent, reversible switching between conductivity states.[8-11] While organic based device have traditionally lagged behind their inorganic counterparts, organic based electrical devices have features that result in competitive advantages over their inorganic counterparts, such as high volume and fast fabrication routes including printing.[12] Recently, organic based memory devices have begun to demonstrate the properties necessary for competing with more established inorganic based systems including nanosecond switching times combined with high endurance and stability.[12] In addition, high performance flexible devices exhibiting artificial synaptic properties have been demonstrated through the use of organic based redox reactions, though these systems require three-terminals to operate.[13,14] Two-terminal artificial synapses have been observed in organic systems using a variety of mechanisms including filamentary conduc-tion,[15] charge transfer,[16,17] and conformational changes.[18,19] This latter mechanism relies on polymers with backbone and/or pendant groups electronic conjugation where field induced conformational changes is the prime process for resistive switching. Resistive switching relies on the molecular mobility of a polymer to allow “islands” of electronic delocalization to spatially readjust to allow charge tunneling or transport between islands under an applied field.[20,21]

As earlier as 1972, a basic understanding of charge transport in the commercially important hole-transporting polymer poly(N-vinyl carbazole) (PVK) was presented.[21] In this polymer, the high hole mobility is due to the pendant carbazole groups where the proper face-to-face alignment of the carbazoles is extremely important for efficient charge transfer. PVK has been shown to have a single conductivity state due to the strict alignment of the carbazole groups along the backbone of the polymer.[18]

However, by making changes to the flexibility of the carbazole groups through alterations of the side chain length that separates the electronically active group from the polymer backbone, the carbazole group can be given enough rotational freedom to undergo conformational changes under electric fields. With this in mind, polymers have been developed which are based on acrylates that have pendant carbazoles and exhibit volatile and non-volatile bistable conductance.[22] One polymer employed as memory is 2-(9H-carbazol-9-yl)ethyl methacrylate (PEMA) where conformational change of the pendant carbazoyl groups is the proposed mechanism in its observed conductance bistability.[18] Once PEMA is switched into its high conductivity state, the electron donating carbazole groups are stabilized by the electron withdrawing ester groups, and the polymer does not return to its off (low conductivity state) when exposed to a reverse bias greater than the switching voltage. Due to its low volatility and propensity to remain in the on state when exposed to a reverse bias as well as over large time scales, this material is categorized as a write-once-read-many (WORM) device. Our group has recently extended this approach to elucidate the effect of chemical structure on the conformationally-induced switching properties of a range of non-conjugated polymers with pendant carbazole moieties. Our specific aim was to explore the role that pendant group flexibility had on switching properties by synthesizing carbazole deri-vatized n-alkyl methacrylate polymers with side chain lengths ranging from n = 2 to n = 11.[23] Increasing the flexibility of the pendant carbazoles results in the transition of a hole-transporting polymer with distinct bistable switching properties to a polymer with an analog switching response that results in tai-lorable multi-state conductance states. One of these latter polymers is appropriate for use as a synaptic substitute, specifically poly(11-(9H-carbazol-9-yl)undecyl methacrylate) (PUMA), and is the focus of the current effort.

2 Results and Discussion

2.1. AC/DC Response

A number of signature characteristics are exhibited by memris-tors in their current-voltage (I-V) response when driven by a bipolar periodic signal such as a hysteresis loop that is pinched at the origin, the area of the hysteresis lobe is a monotonically decreasing function of the excitation signal frequency beyond some frequency, and the I-V response tends to a single-valued function when the excitation frequency tends to infinity.[24] Recently, a range of carbazole-derivatized *n*-alkyl methacrylate polymers were presented by our group, where the *n*-alkyl length ranged from 2 to 11, and it was discovered that a number of memristive characteristics were present in the I-V response of the polymers.[23] These previous studies and the current effort used a simple two-terminal ITO/polymer/Al device structure where the polymer was spin coated on an ITO-coated glass substrate to a thickness of ≈200 nm and then an aluminum electrode was evaporated over the assembly. The "quasi" DC I-V response of the polymers was characterized by the expected erratic & bistable responses.[2] **Figure 1** presents the "quasi" DC I-V response of poly(11-(9H-carbazol-9-yl)undecyl methacrylate) (PUMA) and an obvious "turn-on" voltage (V_{ON}) is evident at ≈4.25 V where the current increases 4 orders of magnitude. Subsequent voltage sweeps did not indicate that the device reset itself as indicative from the 50th and 51st voltage cycle.

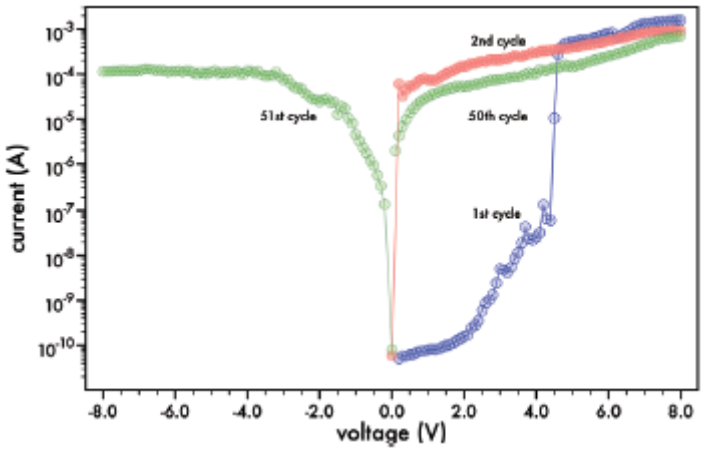

Figure 1. Current-voltage characteristics of PUMA with a V_{DC} sweep from ±8 V. Sweep cycles are labeled. Device was ITO/PUMA/Al and was measured at 23 °C. Voltage varied on Al electrode while ITO was set to 0 VDC.

Initially when the PUMA device is biased at a low positive voltage, holes are injected at the Schottky barrier which is located near the anode (Al) and oxidize the carbazole groups near the interface, forming positively charged species.[18] Spatially adjacent neutral carbazole groups undergo donor-acceptor interactions with the positively charged carbazole groups resulting in rotation of the rings into a partial or full face overlap. This leads to an accumulation of space charge and a redistribution of the electric field.[25] The process is propagated throughout the film and, near the turn-on voltage, a significant fraction of the carbazole groups has undergone such a conformational change. The ordered car-bazole groups, either on neighboring or the same polymer chain, result in an enhanced charge transport through intra- or interchain hopping producing the high conductivity state (ON state). When the device is de-energized, the partial positive charge localized on the carbazoles is stabilized by the electronegative oxygen in the ester linkages.[26] Once the rings have aligned at VON to create a charge carrier pathway, the elevated conductance is not switched off with a reverse bias sweep or with the

application of a higher voltage of the same bias. After transitioning the device to the ON state, the AC I-V response of many of the polymers studied[23] exhibited a pinched hysteresis loop when measured between 1 Hz and a few hundred Hz. For polymers with an *n*-alkyl linkage to the carbazolyl group of $n < 9$, their pinched hysteresis loop was characterized by "jump transitions" indicative of bistability, while polymers with $n \geq 9$ had a pinched hysteresis loop that was smooth in appearance and current values that were an order of magnitude higher at lower driving voltages than polymers with $n < 9$.

In these polymers, charge carriers are assumed to have a higher intra- & inter-chain mobility when the overlapping of related orbitals is large between two adjacent carbazoles.[27,28] The transition from a bistable to a continuously variable response is due to the increased flexibility of the pendant carbazoles. Achieving this overlap is directly related to the local electric field that the moieties experience that force them to adopt an overlapping conformation, as well as their rotational activation energy. Dielectric spectroscopy indicated that as the *n*-alkyl length is increased, the rotation flexibility of the carbazole moiety is enhanced, with the activation energy dropping from 681 kJ mol^{-1} for $n = 2$ to 196 kJ mol^{-1} for $n = 11$.

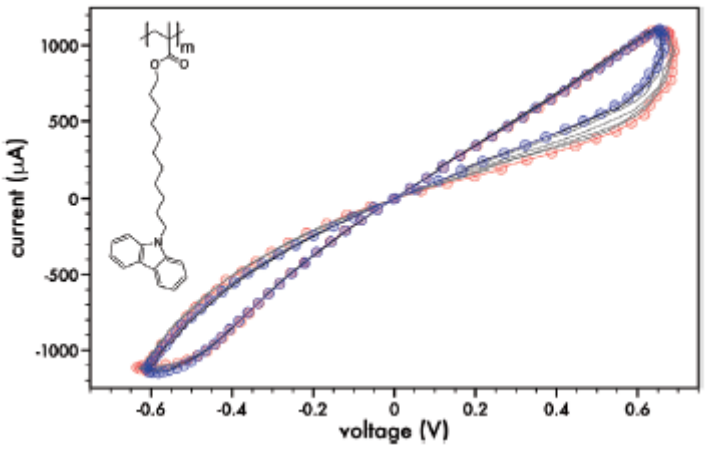

Figure 2. Current-voltage characteristics of PUMA (structure inset) with sinusoidal input (V_{AC}) at a frequency of 20 Hz. 10 full cycles across the device are presented and, specifically, the 1st (red circle) and 10th cycle (blue circle) are labeled.

Figure 2 prese nts the AC response of PUMA under a sinusoidal driving voltage (V_{AC}) at a frequency of 20 Hz. The devices were initially "turned on" by exposing them to a train (≥5) of waveforms prior to testing. The ten full cycles across the device after being turned on are presented and, specifically, the 1st (red circle) and 10th cycle (blue circle) are labeled. This polymers exhibit a pinched hysteresis loop that tends to single-valued function when the excitation frequency tends to infinity.[23] The glass transition temperature (T_g) of the polymer is slightly below the testing temperature of 23 °C with PUMA having a T_g of 14 °C. The hysteresis loop of PUMA exhibits smooth and successive current transitions between increasing driving voltages and differs greatly from other *n*-alkyl methacrylate polymeric memristors or their derivatives when the *n*-linkage is under 6 units. These latter polymers exhibited a pronounced "bistability" in their electrical response. [18,23] As indicated in **Figure 1**, the repetitive and immediate DC cycling of the polymer did not result in the device resetting itself, though if the device was switched on and then allowed to rest for a few hours under ambient conditions with no electric field, the polymer would slowly begin to exhibit a reduced current flow as if the device was resetting itself. **Figure 3** presents the DC I-V response of a device that was "turned-on", allowed to age under no bias, and then again exposed to a DC bias from 0 V_{DC} to 8 V_{DC}. Within 12 hours of aging, the device

exhibits a 97 % drop in supported current at 1 V_{DC}. The inset in **Figure 3** presents the current at 1 V_{DC} bias over eight days of aging and indicates that there is over a three-order of magnitude drop in supported current. This slow resetting is indicative of the polymer's low glass transition temperature relative to the ambient conditions which allows the polymer to reorganize and possibly allow the carbazole rings to become uncorrelated, disrupting charge transfer. To investigate this relaxation further, a thermally stimulated depolarization current (TSDC) study was conducted, where **Figure 4** presents the depolarization current of PUMA with a temperature scan after the sample was poled. In this technique, the 0.25 mm thick material is sandwiched between two electrodes and heated to 90 °C under an applied voltage (50 V_{DC}). The sample was then cooled while maintaining the electric field on the sample. Once -75 °C was reached, the electric field was removed and the sample was heated at a rate of 1 °C min^{-1}, while monitoring the current.

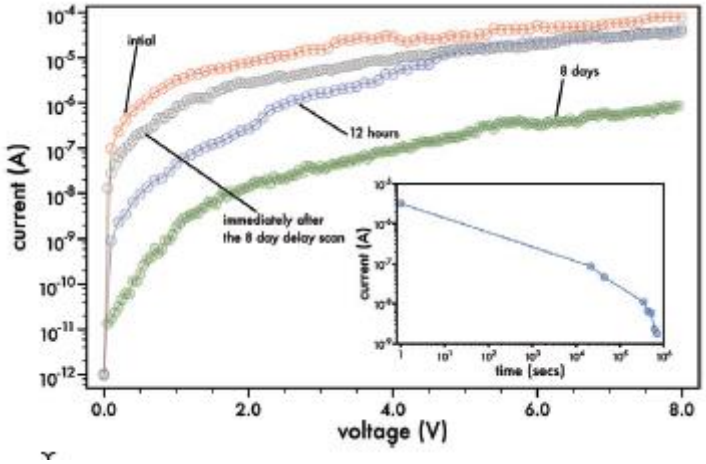

Figure 3. Current-voltage characteristics of PUMA with a V_{DC} sweep from 0 to 8 V after an aging period. Sweep cycles are labeled. Inset presents the supported current at a 1 V_{DC} bias. Both electrodes were tied to ground during the aging period. Device was ITO/PUMA/Al and was measured at 23 °C.

In **Figure 4**, there is no measurable current flow in the sample from -75 °C up to ≈10 °C, whereupon there is a dramatic 3-orders of magnitude increase in current flow. Once the field is removed and the sample is warmed, PUMA can become depolarized at a temperature that is correlated to the activation energy for large-scale chain mobility, resulting in an observable current flow through the sample. The increase in chain flexibility agrees well with the 14 °C DSC-derived glass transition temperature of the polymer. Based on these results, it is clear that electrical testing of PUMA at room temperature (23 °C) is in a temperature regime where there is significant charge mobility based on the flexibility of the polymer backbone.

2.2. Multiconductance States

To further establish the ability of PUMA to sample a range of conductance states, a device was exposed to a train of excitatory voltage pulses after being set to the ON state. The pulse train starts at an absolute value of 4 V_{DC} with each subsequent pulse being increased by an absolute value of 0.25 V, so that the final absolute value of the pulse is 5 V_{DC}. The train consists of the positive and negative polarity of the pulse being applied to the aluminum electrode of the device while the ITO electrode was maintained at zero potential.

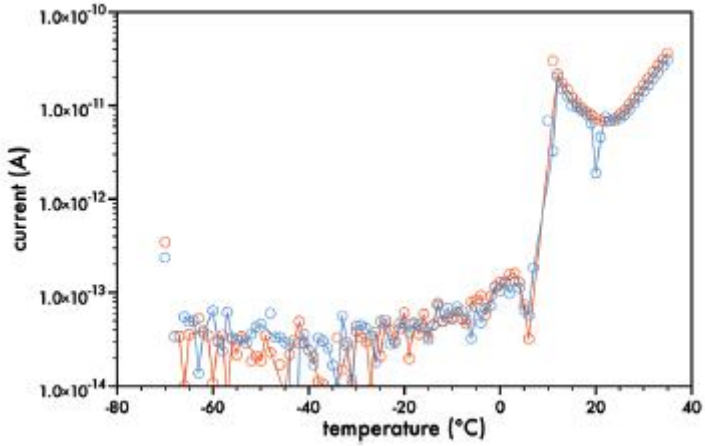

Figure 4. Thermally stimulated current (TSC) of poled PUMA. Two different temperature scans are presented.

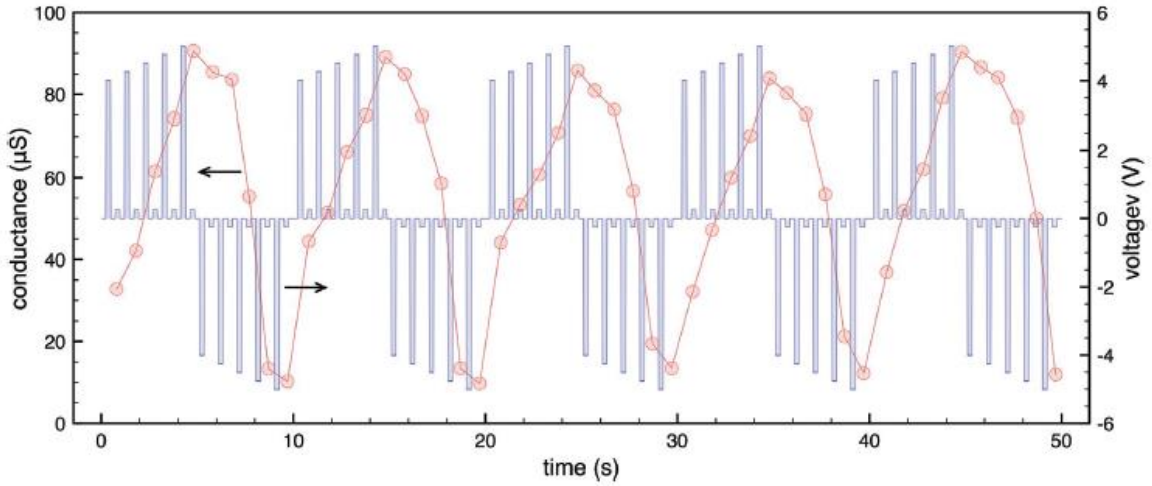

Figure 5. Conductance of PUMA device with varying excitatory voltage pulses. The voltage pulses were 240 ms in duration and occurred every 720 ms. A conductance measurement pulse of 0.25 V (240 ms duration) was applied 240 ms after the end of the excitatory voltage pulse. Device was ITO/ PUMA/Al and was measured at 23 °C.

The voltage pulses were 240 ms in duration and occurred every 720 ms, while a conductance measurement pulse of 0.25 V_{DC} (240 ms duration) was applied 240 ms after the end of the excitatory voltage pulse. **Figure 5** presents the pulse pattern and resulting conductance of the PUMA device. The conductance of the sample varies approximately from a high value of 90 µS at the end of the positive voltage pulse segment to a minimum of 10 µS at the end of the corresponding negative voltage pulse segment. The conductance values track relatively well with each excitatory pulse, though the absolute change between each pulse is different between the positive and negative pulses.

Figure 6 presents the average and standard deviation of the conductance across a typical 50 pulse train. The positive pulses result in a relatively linear increase in conductance with each pulse increasing by ≈12 µS while the decrease in conductance with the negative pulses is sigmoidal in shape. The difference in shape between the ascending and descending conductivity values is reflected in the low standard deviation in the ascending values while the descending values have a large standard deviation after the second negative pulse (cf. **Figure 6**).

The voltage-pulse train response of a PUMA-based device to a number of consecutive pulses was studied in order to assess the saturation effects of the device. Figure 7 presents the current response of a device to 50 consecutive pulses with a 275 ms duration and spaced 275 ms apart. Initially, the device was set to the ON state through a -8 V_{DC} to 8 V_{DC} sweep then was exposed to stream of 50 consecutive -6 V_{DC} pulses. The resulting current response in the device was a gradual increase in current from 0.1 µA to a saturated value of 2.01 µA, a 20-fold increase. Pulsing the device with more than 50 consecutive pulses did not appreciably increase the current. Reversing the polarity and pulsing the device with 6 V_{DC} train resulted in the immediate drop in current to ≈0.3 µA and then a gradual drop to 0.05 µA at the end of the pulse train. The increase in current flow with consecutive pulses and then reduction with reverse polarity pulses could be achieved if the pulses where initially positive or negative. It appears that for devices that have not ever been biased before, that an initial pulsing, either positive or negative, tends to enhance percolative paths. This enhancement is then disrupted if reverse voltage pulses are applied to the device.

The energy difference between the HOMO (-5.67 eV) and LUMO (-2.16 eV) of PUMA and the work function of the metal electrodes (ITO = -4.7 eV,[29] Al = -4.3 eV) will result in Schottky barriers being formed at both interfaces.[25] The negative voltage sweeps with ITO as the anode, holes are injected from the ITO electrode and electrons are injected from the Al electrode.

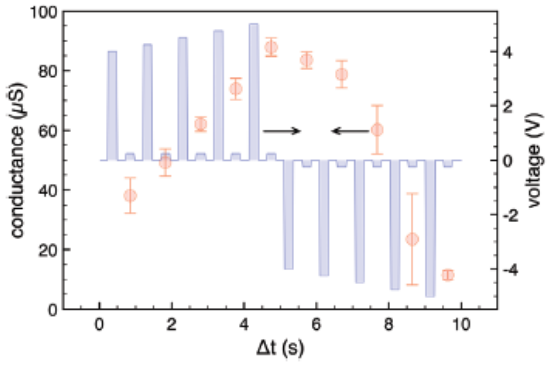

Figure 6. Conductance of PUMA device with varying excitatory voltage pulses. The voltage pulses were 240 ms in duration and occurred every 720 ms. A conductance measurement pulse of 0.25 V (240 ms duration) was applied 240 ms after the end of the excitatory voltage pulse.

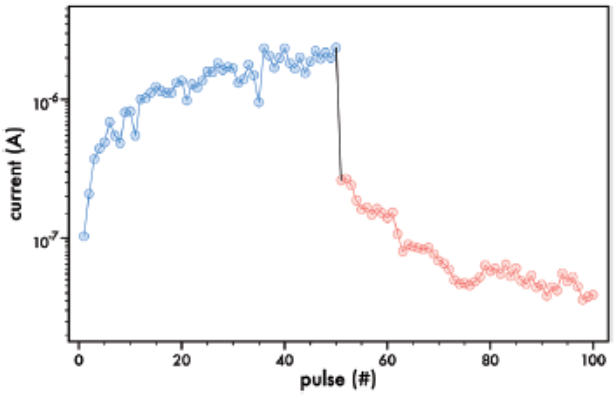

Figure 7. Current response of PUMA device after 50 consecutive negative pulses (V_{DC} = -6 V, 275 ms) and then 50 consecutive positive pulses (V_{DC} = 6 V, 275 ms). Device was ITO/PUMA/Al and was measured at 23 °C. Voltage varied on Al electrode while ITO was set to 0 V_{DC}.

The energy barrier at the ITO/PUMA (HOMO level) contact is relatively low at 0.97 eV, when compared to the 2.14 eV barrier at the Al/PUMA (LUMO level) contact. In contrast, positive voltage sweeps result in the Al electrode acting as the anode. In this configuration, the energy barrier to holes at the Al/PUMA contact is 1.37 eV while electrons are injected from the ITO/PUMA interface through a 2.54 eV barrier. Based on these energy differences, one would expect that positive/ negative voltage pulses would result in some level of asymmetry in the resulting current.

2.3. Spike-Timing-Dependent-Plasticity (STDP)

Due to its ability to smoothly transition across a range of conductivity states with voltage pulses, PUMA was taken as the candidate for further study as a synaptic substitute. One of the fundamental characteristics of synaptic plasticity in biological neural networks is spike-timing-dependent-plasticity (STDP) and its replication in a synthetic model is critical for emulating biological systems.[9,30,31]

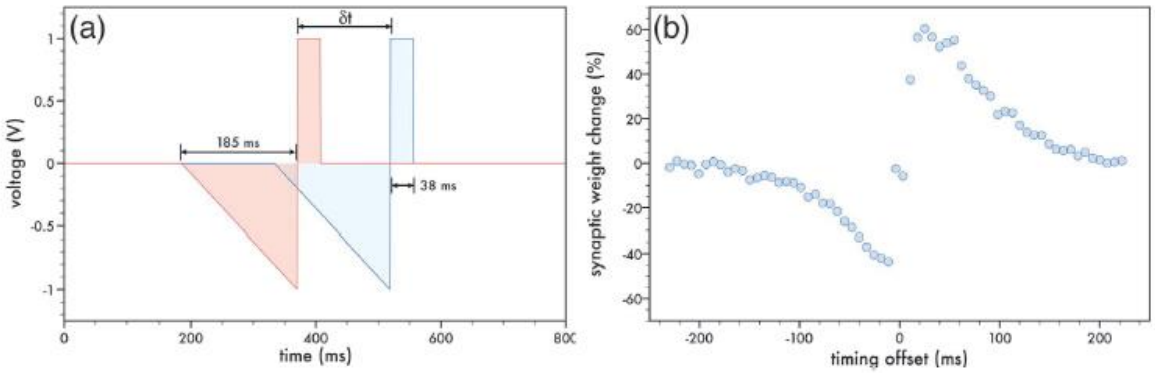

Figure 8. Spike-timing-dependent-plasticity (STDP) of PUMA. a) Profiles of the presynaptic (blue) and postsynaptic (red) spikes with ±1 V peak height and 223 ms total duration, while the timing offset between the spikes is labeled. b) Synaptic weight change with the variation in timing offset between the presynaptic and postsynaptic spike-pair. Device was ITO/PUMA/AL and the presynaptic and postsynaptic spike was applied to the ITO and aluminum electrode, respectively.

STDP can be viewed as a spike-based formulation of a Hebbian learning rule where the strength of connections between neurons is modulated by the relative timing of the output and input action potentials (spikes) to the neurons. STDP has been demonstrated in multiple species, including humans, and is considered the basis for cognitive learning.[31-34] The STDP response of an ITO/PUMA/Al memristor is presented in Figure 8 where the ITO and aluminum electrodes were designated the presynaptic and postsynaptic neuron, respectively. Using presynaptic and postsynaptic spikes with a voltage profile as presented in Figure 8a, the potentiation and depression of the synaptic weight could be modulated with a variation in the timing offset of the two pulses. The synaptic weight change (ΔW) was calculated as $\Delta W = (\sigma_2 - \sigma_1)/\sigma_1$ where σ_1 and σ_2 was the conductivity of the device prior to and 1s after the application of the presynaptic and postsynaptic spikes, respectively; the conductivity sensing was determined by averaging the conductance of five 0.2 V sensing pulses. The device conductivity was measured after a train of five pulses were applied to the device to mimic biological systems where a train of spikes have been observed to elicit enhanced synaptic weight changes.[35] In **Figure 8b**, when the presynaptic spike arrives before the postsynaptic spike, there is a potentiation of the synaptic weight (ΔW) while depression occurs when the presynaptic spike arrives after the postsynaptic spike.

This response is similar to a Asymmetric Hebbian Learning Rule, where leads to long-term potentiation (LTP) of the synapse and leads to long-term depression (LTD) of the synapse.

2.4. Flexible Devices

A clear advantage with polymeric devices is the inherent mechanical flexibility of the device when the active material is deposited on a flexible substrate.[36] Substituting ITO-coated poly(ethylene terephthalate) (PET) films for the glass substrate of the devices, fully flexible PUMA devices were constructed and repetitively bent over a 14 mm diameter cylinder.

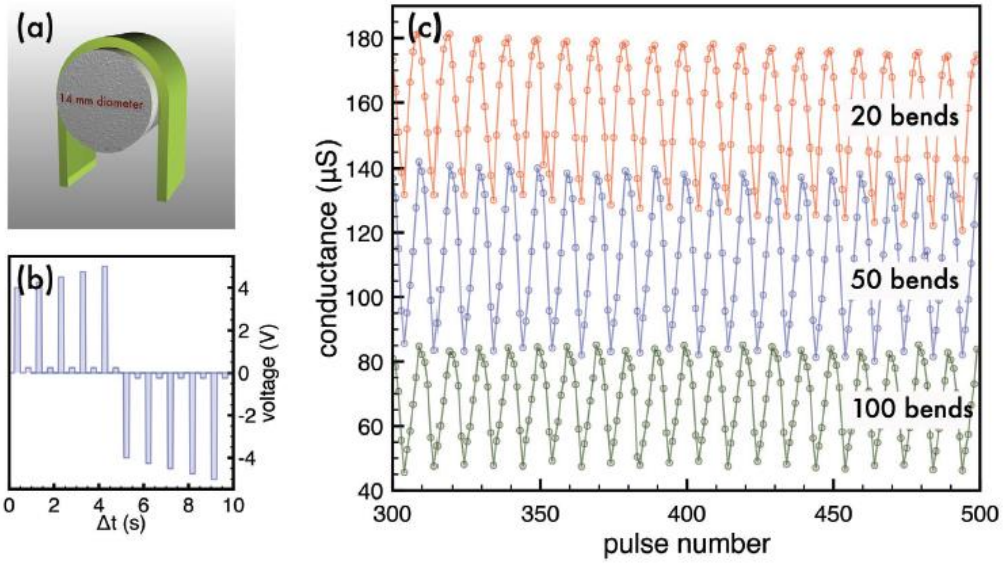

Figure 9. The electrical response of a flexible PUMA memristive device was investigated by a) wrapping the device around a 14 mm diameter rod a number of times and then performing standard conductance change with voltage pulsing. b) Voltage excitation waveform input to device and c) Conductance variations of device with 20 (red), 50 (blue), and 100 (green) bends. Curves shifted for clarity.

Figure 9a presents a schematic of the bending jig; devices were repetitively bent and then subjected to electrical testing. Figure 9c presents the conductance of the PUMA device, after 20, 50, or 100 bending cycles, to a train of excitatory voltage pulses which had the profile presented in Figure 9b. The samples used for the bending study exhibited similar initial conductivities after the devices were set to the ON state (cf. Figure 1) and, as indicated in Figure 9c, the peak-to-peak change in conductance of all the samples was on the order of 30-45 μS after 500 pulses. As discussed previously in Figure 6, the positive pulses result in a relatively linear increase in conductance with each pulse while the decrease in conductance with the negative pulses is sigmoidal in shape. Specifically looking at the sample that underwent 100 bending cycles in Figure 10a, which presents the average and standard deviations in conductance, this linear/sigmoidal response is evident. Surprisingly, the error associated with each conductance point is less than 1 % of the average value. The conversion of the conductance to a triangular form (cf. Figure 10b) requires a transform function that is presented in Figure 10c. For positive pulses (pulses 1-6), the transform function has a maximum value of 4% shift to adjust the raw conductance to achieve a linear response, while on on the negative pulses (pulses 7-11), the maximum shift is 14%.

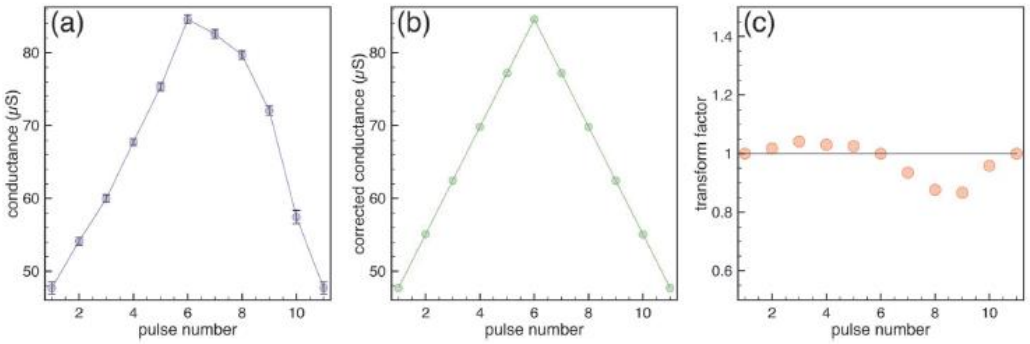

Figure 10. Conductance ofPUMA device with varying excitatory voltage pulses after 100 bending cycles (cf. Figure 9): a) average and standard deviation of conductance, b) "corrected" conductance, and c) transform function.

3. Conclusion

The electrical properties of a carbazole derivativized methacrylate polymer were investigated in order to assess its value as an artificial synapse. Specifically, poly(11-(9H-carbazol-9-yl)undecyl methacrylate) (PUMA) exhibited a number of signature memristor characteristics such as an abrupt and irreversible transition from an insulator to a conductor at a specific DC voltage and a phase shifted output relative to a sinusoidal input resulting in hysteresis in the AC response. A PUMA-based device could transition through a multitude of conductance states with varying voltage, allowing the device to exhibit spike-timing-dependent-plasticity (STDP). Equating the change in conductance across the PUMA-based device with synaptic weight, long-term potentiation (LTP) and long-term depression (LTD) were demonstrated with the artificial synapse.

4. Experimental Section

Materials: Commercial reagents were purchased and were used without further purification. All the solvents were dried according to standard methods. Deionized water was obtained from a Nanopure System and exhibited a resistivity of $\approx 10^{18}$ Ohm^{-1} cm^{-1}. The synthesis of poly(11-(9H-carbazol-9-yl)undecyl methacrylate) (PUMA) has been presented previously.[23]

Device Formation: The devices were fabricated on unpolished float glass measuring 12.7 mm x 12.7 mm x 0.7 mm with one side coated in ITO with a sheet resistance of 8-12 Ω. The ITO anode was masked with a piece of vinyl tape with a width of 4 mm in the center of the slide for the full length (12.7 mm). The uncovered ITO was then etched away using a metal-acid reaction with zinc powder (Fisher Scientific) and highly concentrated HCL (36.5% to 38%) (VWR). The slides were then washed with deionized (DI) water, and the tape is removed. The sample was further cleaned by sonicating the sample in acetone for 10 min before being wiped with a non-sterile cotton tip swab (Fisher Scientific) and sonicating in isopropyl alcohol for 10 min. The sample was dried under nitrogen, loaded into a Harrick plasma cleaner/sterilizer PDC-32G, and run on the high setting for 5 min. The desired polymer was dropped onto the anode from a solution of chlorobenzene (Acros) at a concentration of 50 mg mL^{-1} and spun at 2000 rpm in a Specialty Coating Systems Spincoat G3P-8 resulting in a film with a thickness of approximately 200 nm. The samples were then placed into a Denton Vacuum DV-502A evaporation chamber with an aluminum pellet (Kurt J. Lesker 1/4 in diameter x 1/2 in length) in a tungsten basket heater coil (Kurt J. Lesker). A mask was used to create two aluminum strips that are perpendicular to the ITO strip such that there are two devices per sample, each having and area of 16 mm^2. The chamber was allowed to pump down to approximately 2 x 10^{-6} torr. The aluminum was then evaporated until the thickness of the electrode was approximately 200 nm as measured by a Sigma Instruments SQM-160 rate/thickness monitor.

Device Testing: The AC tests were performed on a custom setup that utilized an Agilent 33120A 15 MHz function/arbitrary waveform generator to generate the signal and a National Instruments PCI-6013 data acquisition (DAQ) board to measure the output signals. A breadboard was constructed such that the memristor was in series with a resistor as a traditional voltage divider. The signal was run through the memristor and standard resistor, and the voltage drop across the standard resistor was measured. The signal was initially fed into the aluminum electrode of the memristor and traveled through the standard resistor which is also tied to ground.

For the application of the presynaptic and postsynaptic pulses, the same setup was used, but a relay was incorporated in such a way that the setup can function as previously described but with the device floating.

DC conductivity and saturation studies were performed with a HP 4145A Semiconductor Parameter Analyzer coupled to a HP 16058A Test Fixture. The ITO electrode was maintained at 0 V during testing while the potential on the aluminum electrode was varied.

Thermally Stimulated Current: Thermally stimulated current (TSC) studies were performed on a Novocontrol Broadband Dielectric/ Impedance Alpha-A Quatro Series Spectrometer. Samples were sandwiched between an upper and lower electrode that was 20 mm in diameter. The procedure was to place the polymer between the electrodes under a slight load, place the assembly into the spectrometer, and heat the sample up past its glass transition; this resulted in a film thickness of ≈200-300 µm. A 50 V DC voltage was then applied and the sample was then cooled to -75 °C. The voltage was then set to 0 V and the sample was then heated at a rate of 1 °C min^{-1} under a nitrogen purge while monitoring the current.

Reference

[1] L. O. Chua, IEEE Trans. Circuit Theory 1971, Ct18, 507.

[2] L. Chua, Applied Physics a-Materials Science & Processing 2018, 124, 43.

[3] D. B. Strukov, G. S. Snider, D. R. Stewart, R. S. Williams, Nature 2008, 453, 80.

[4] A. Szymanski, D. C. Larson, M. M. Labes, Appl. Phys. Lett. 1969, 14, 88.

[5] J. Kevorkia, M. M. Labes, D. C. Larson, D. C. Wu, Discuss. Faraday Soc. 1971, 139.

[6] A. R. Elsharkawi, K. C. Kao, J. Phys. Chem. Solids 1977, 38, 95.

[7] L. Chua, Semicond. Sci. Technol. 2014, 29.

[8] Y. Li, Y. P. Zhong, L. Xu, J. J. Zhang, X. H. Xu, H. J. Sun, X. S. Miao, Sci. Rep. 2013, 3.

[9] Y. Li, Y. P. Zhong, J. J. Zhang, L. Xu, Q. Wang, H. J. Sun, H. Tong, X. M. Cheng, X. S. Miao, Sci. Rep. 2014, 4.

[10] T. H. Lee, S. R. Elliott, Phys. Rev. B 2011, 84.

[11] S. Kim, J. Park, S. Jung, W. Lee, J. Woo, C. Cho, M. Siddik, J. Shin, S. Park, B. H. Lee, H. Hwang, Appl. Phys. Lett. 2011, 99.

[12] S. R. Forrest, Nature 2004, 428, 911.

[13] S. Goswami, A. J. Matula, S. P. Rath, S. Hedstrom, S. Saha, M. Annamalai, D. Sengupta, A. Patra, S. Ghosh, H. Jani, S. Sarkar, M. R. Motapothula, C. A. Nijhuis, J. Martin, S. Goswami, V. S. Batista, T. Venkatesan, Nat. Mater. 2017, 16, 1216.

[14] Y. van de Burgt, E. Lubberman, E. J. Fuller, S. T. Keene, G. C. Faria, S. Agarwal, M. J. Marinella, A. A. Talin, A. Salleo, Nat. Mater. 2017, 16, 414.

[15] S. La Barbera, D. Vuillaume, F. Alibart, Acs Nano 2015, 9, 941.

[16] H. Tian, X. Cao, Y. J. Xie, X. D. Yan, A. Kostelec, D. DiMarzio, C. Chang, L. D. Zhao, W Wu, J. Tice, J. J. Cha, J. Guo, H. Wang, Acs Nano 2017, 11, 7156.

[17] C. Wang, G. Liu, Y. Chen, R. W. Li, W. B. Zhang, L. X. Wang, B. Zhang, J. Mater. Chem. C 2015, 3, 664.

[18] S. L. Lim, Q. D. Ling, E. Y. H. Teo, C. X. Zhu, D. S. H. Chan, E. T. Kang, K. G. Neoh, Chemistry of Materials 2007, 19, 5148.

[19] G. Liu, B. Zhang, Y. Chen, C. X. Zhu, L. J. Zeng, D. S. H. Chan, K. G. Neoh, J. N. Chen, E. T. Kang, J. Mater. Chem. 2011, 21, 6027.

[20] W. Klopffer, J. Chem. Phys. 1969, 50, 2337.

[21] W. D. Gill, Journal ofApplied Physics 1972, 43, 5033.

[22] Y. K. Fang, C. L. Liu, W. C. Chen, J. Mater. Chem. 2011, 21, 4778.

[23] T. M. McFarlane, B. Zdyrko, Y. Bandera, D. Worley, O. Klep, M. Jurca, C. Tonkin, S. H. Foulger, J. Vilcakova, P. Saha, J. Pfleger, J. Mater. Chem. C 2018, 6, 2533.

[24] S. P. Adhikari, M. P. Sah, H. Kim, L. O. Chua, Ieee Transactions on Circuits and Systems I-Regular Papers 2013, 60, 3008.

[25] Q. D. Ling, Y. Song, S. L. Lim, E. Y. H. Teo, Y. P. Tan, C. X. Zhu, D. S. H. Chan, D. L. Kwong, E. T. Kang, K. G. Neoh, Angewandte Chemie-International Edition 2006, 45, 2947.

[26] G. Safoula, K. Napo, J. C. Bernede, S. Touihri, K. Alimi, Eur. Polym. J. 2001, 37, 843.

[27] P. C. Johnson, H. W. Offen,J. Chem. Phys. 1971, 55, 2945.

[28] D. J. Williams, W. W. Limburg, J. M. Pearson, A. O. Goedde, J. F. Yanus,J. Chem. Phys. 1975, 62, 1501.

[29] J. S. Kim, M. Granstrom, R. H. Friend, N. Johansson, W. R. Salaneck, R. Daik, W. J. Feast, F. Cacialli, J. Appl. Phys. 1998, 84, 6859.

[30] S. Z. Li, F. Zeng, C. Chen, H. Y. Liu, G. S. Tang, S. Gao, C. Song, Y. S. Lin, F. Pan, D. Guo, J. Mater. Chem. C 2013, 1, 5292.

[31] L. F. Abbott, S. B. Nelson, Nat. Neurosci. 2000, 3, 1178.

[32] N. Caporale, Y. Dan, Annual Rev. Neurosci. 2008, 31, 25.

[33] S. Cassenaer, G. Laurent, Nature 2007, 448, 709.

[34] D. E. Feldman, Neuron 2012, 75, 556.

[35] R. C. Froemke, Y. Dan, Nature 2002, 416, 433.

[36] J. A. Rogers, T. Someya, Y. Huang, Science 2010, 327, 1603